Oviedo
(Spain)
1-3 July
2008
International Meeting of Young Researchers
in Structural Geology and Tectonics

*O R S G E T*

# Prediction of stress fields in accretionary wedges by optimization

P. Souloumiac[1, 2*], A. Modaressi-Farahmand-Razavi[1] and Y. M. Leroy[2]

[1]*Laboratoire MSS-Mat, CNRS UMR 8579, Ecole Centrale Paris, Châtenay Malabry, France.*

[2]*Laboratoire de Géologie, CNRS, Ecole Normale Supérieure, Paris, France.*

*e-mail: souloumiac@mailhost.geologie.ens.fr*

**Abstract:** The objective is to propose a simple procedure, compared to the finite-element method, to select and optimize the dominant mode of thrusting in accretionary wedges. The methodology, referred to as the Equilibrium Element Method (EEM), is an application of the internal approach of limit analysis, which leads to the determination of the lower boundary on the tectonic force and the associated optimal stress distribution. The EEM has the advantage of requiring only a fraction of the computational power necessary for the FEM.

**Keywords:** limit analysis, finite elements, accretionary wedges, stress distributions, tectonic force.

This research is part of an effort to account for mechanical equilibrium and material strength in geometrical models of folds. Cubas *et al.* (2008) have shown that the external approach of limit analysis (Salençon, 2002) could be applied to thrusting, providing the means to assess the lifetime of a thrust fold and to construct sequences of folds while keeping the geometrical simplicity of the constructions proposed in the seminal work of Suppe (1983). This complementary project is aimed at constructing statically admissible stress fields at any step of the development of these structures. The EEM, which is inherited from the internal approach of limit analysis, has been shown by Souloumiac *et al.* (2009), to be applicable to these geological structures, as illustrated here for the case of an accretionary wedge.

**The Equilibrium Element Method**

The EEM is the systematic application of the internal approach by numerical means (Pastor, 1978). It provides the lower boundary in the tectonic force as well as the optimal stress field satisfying equilibrium and the limited strength of the materials. The example of

the wedge is chosen to illustrate the feasibility of this method for geological structures, an example of a single wedge being presented in figure 1. The wedge OADCB of height $H$ either slides over the weak décollement (OB) or faults internally. The angle $\beta$ is the dip of the décollement and thus the angle between gravity and the $y$ axis. The tectonic force $F$ results from a linear distribution of the stress along the left boundary OA. The topography has a slope $\alpha$ from A to D and is flat from D to C.

The domain OADCB is discretized with crossed triangles as illustrated in figure 1. Each triangular element provides a linear stress distribution with nodal unknowns: the three stress components ($\sigma_x$, $\sigma_y$, $\sigma_{xy}$).

The components of the optimal stress field are chosen within a set of statically admissible (SA) stress fields which satisfy the following two conditions (Salençon, 2002). First, mechanical equilibrium must be enforced over the domain and its boundary. Mechanical equilibrium leads to a set of two equations over each triangular sub-domain. It leads also along the three sides of each triangular element
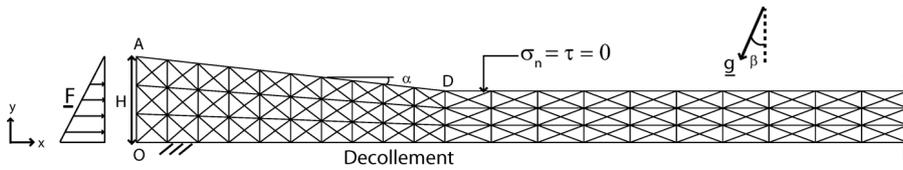
**Figure 1.** Geometry of an accretionary wedge.

(except at the boundary of the domain) to two equations to enforce the continuity of the stress vector, leading to jumps in certain components of the stress vector. To this end, two collapsed triangles are attached to each side of an equilibrium element as shown in figure 2. Krabbenhøft *et al.* (2005) have shown that once a triangle has collapsed, so having zero surface, writing the two equilibrium equations is equivalent to writing the jump conditions.

At the boundary, the stress vector must be equal to the distributed load defining the boundary conditions. As shown in figure 1, surface AC is stress-free and the normal stress on side AO has an imposed linear gradient with depth.

The second condition on the SA stress field is that it must remain in the convex strength domain at every point of domain $\Omega$ and along major discontinuities such as the décollement. This strength domain is bounded by the Coulomb criterion (cohesion $c$ and friction angle $\Phi$) in our case. The linearity of the stress interpolation means that if such constraint is



**Figure 2.** Illustration of the two collapsed triangular elements proposed by Krabbenhøft *et al.* (2005).

respected at the three nodes, it is respected over the whole element.

The equilibrium and the limitation of the strength domain lead to a set of linear equations and inequalities for the nodal stresses. The objective function of this optimization problem corresponds to the force $\underline{F}$

which is to be maximised. Here, it is the gradient which needs to be maximised. The result of this optimization is the value of the lower boundary on the tectonic force.

The set of equalities and inequalities is constructed with the standard finite-element code SARPP (2007), which has been extended for the Equilibrium Elements Method. The optimization problem is solved with the commercial package MOSEK (2007), throughout the rest of this contribution. The next part presents the results obtained for an accretionary wedge.

## Applying the EEM to the Nankai accretionary wedge

The objective is now to apply the EEM to the Nankai accretionary wedge, on the SE coast of Japan, which has the geometrical parameters presented in figure 3. This 2D structure has been interpreted by Moore *et al.* (1991) from the seismic profile NT62-8. The cohesion $c_D$ and the friction angle $\Phi_D$ are the specific properties of the total décollement and the cohesion $c_B$ and the friction angle $\Phi_B$ are those of the bulk material. The other boundary conditions are the same as the boundary conditions described in figure 1. Figure 3 also shows the mesh with triangular elements described in figure 2. This mesh is refined with 12,720 elements (including collapsed elements for the stress discontinuities) and 9640 nodes.

The first result, presented in figure 4, is the failure mode for a value of the friction angle on the décollement $\Phi_D = 9°$. It is analyzed with the distance to Coulomb's criterion, in a scale varying from zero to one. If the stress state exactly satisfies the criterion, the scaled distance is equal to zero (white color). If the stress state is at a distance of 3% from the stress reference, the distance is one (black color).

The incipient thrust is approximately where predicted by Morgan and Karig (1995) and Cubas *et al.* (2008), although the EEM value of the friction angle on the décollement ($\Phi_D = 9°$) is smaller than the one found in the latter contribution ($\Phi_D = 11°$). The ramp dips at 30° and the associated thrust dips at 35°. A second thrust appears that corresponds to a small topograph-

bulk material ($c_B$ =1MPa , $\phi_B$= 30° )

200m

300m

decollement ($c_D$= 0MPa , $\phi_D$ = 9°)

Gravity = 9.81 m/s², Mass density = 2200 Kg/m³, Dip of the decollement = 1.3°
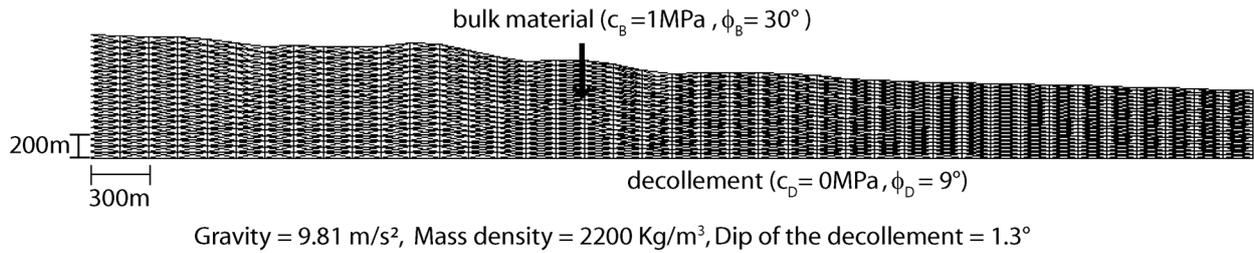
**Figure 3.** The mesh with triangular elements over the section through the Nankai wedge used for the EEM and parameters.

0.8
0.6
0.4
0.2

**Figure 4.** The failure mode illustrated with the distance to the Coulomb criterion for a friction angle of $\Phi_D$ = 9°.

ic perturbation. The décollement is used as far as the base of the major ramp represented in figure 4.

The second result, presented in figure 5, concerns the distribution of principal stresses in the wedge. The EEM directly provides the values of optimal stresses at each node of the mesh. The optimal stress field is presented for a friction angle on the décollement of 9°. The first plot represents the distribution of the quantity: $(\sigma_I - \sigma_{II})/2$, the values ranging from 0 on the top surface to 30 MPa in the left corner at the décollement. The second plot shows the distribution of the quantity: $(\sigma_I + \sigma_{II})/2$, the values ranging from -60 MPa in the bottom left-hand corner to 0 on the top surface. This plot shows the influence of the surface topography on the stress distributions.

The third result obtained by the EEM is the value of the lower boundary on the tectonic force, which is

59.82 GN for $\Phi_D$ = 9°. These calculations take only a few minutes with the optimization software MOSEK (2007) on a personal computer. So the EEM is an efficient method (in terms of CPU time) to provide the stress distribution, the shape of the bulk failure and the lower boundary in the tectonic force.

**Discussion and conclusion**

The objective of this paper is to present a numerical solution to the internal approach of limit analysis, referred to as the Equilibrium Element Method. This method is applicable to complex geometries with major discontinuities such as a décollement. It is a powerful tool for constructing the stress distribution with short calculation times. This optimal stress field is valid at any step of the development of folding. The evolution of the system is predicted by the kinematics approach (Cubas *et al.*, 2008) based

$(\sigma_I - \sigma_{II})/2$

[MPa]

0   10   20   30

$(\sigma_I + \sigma_{II})/2$

[MPa]

-50         0
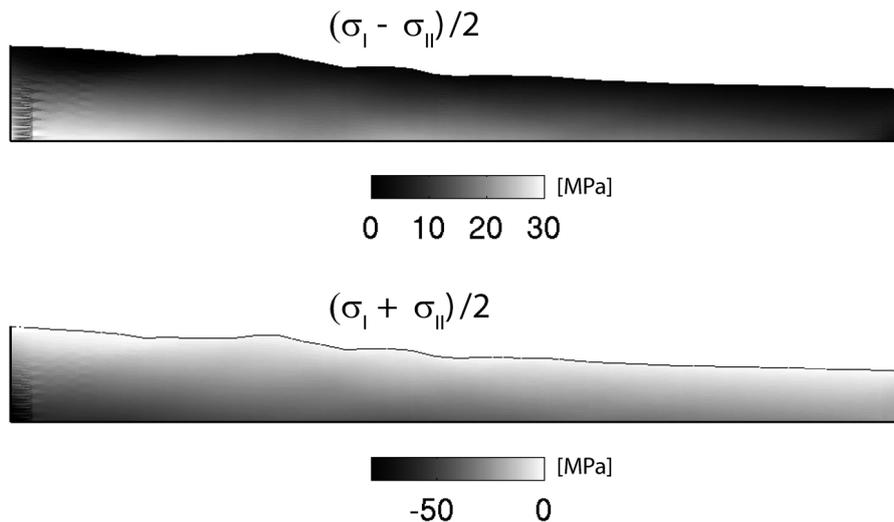
**Figure 5.** Distribution of difference of principal stresses for a friction angle of $\Phi_D$ = 9°.

on the external approach of the limit analysis. So the EEM is complementary to the external approach. Application of the two procedures to an evolving fold provides the stress distributions over the optimized structure, as well as an error estimate for the tectonic force.

## References

Cubas, N., Leroy, Y. M. and Maillot, B. (2008): Prediction of thrusting sequences in accretionary wedges. *J. Geophys. Res.*, 113: B12412. doi:10.1029/2008JB005717.

Krabbenhøft, K., Lyamin, A. V., Hjiaj, M. and Sloan, S. W. (2005): A new discontinuous upper bound limit analysis formulation. *Int. J. Numer. Meth. Eng.*, 63: 1069-1088.

Moore, G. F., Karig, D. E, Shipley, T. H., Taira, A., Stoffa, P. L. and Wood, W. T. (1991): Structural framework of the ODP leg 131 area, Nankai's through. *Proceeding of the Ocean Drilling Program, Initial reports*, 131: 15-20.

Morgan, J. K. and Karig, D. E. (1995): Kinematics and a balanced and a restored cross-section across the toe of the eastern Nankai accretionary prism. *J. Struct. Geol.*, 17: 31-45.

MOSEK (2007): *MOSEK optimization software*. World Wide Web address: http://www.mosek.com.

Pastor, J. (1978): Limit analysis: numerical determination of complete statical solutions. Application to the vertical cut (in French). *J. Méc. Appl.*, 2: 168-196.

Salençon, J. (2002): *De l'Élasto-plasticité au Calcul à la rupture*. Editions de l'École Polytechnique, Paris, 262 pp.

SARPP (2007): *Structural Analysis and Rock Physics Program*, École Normale Supérieure, Paris.

Souloumiac, P., Leroy, Y. M., Maillot, B. and Krabbenhøft, K. (2009): Predicting stress in fold and thrust belts and accretionary wedges by optimization. *J. Geophys. Res.,* 114, B09404, doi: 10.1029/2008JB005986.

Suppe, J. (1983): Geometry and kinematics of fault-bend folding. *Am. J. Sci.*, 283, 7: 684-721.